

- (9) J. J. Toulme and C. Hélène, *J. Biol. Chem.*, **252**, 244–249 (1977).  
 (10) N. C. Seeman, J. M. Rosenberg, and A. Rich, *Proc. Natl. Acad. Sci. U.S.A.*, **73**, 804–808 (1976).  
 (11) C. Hélène, *FEBS Lett.*, **74**, 10–13 (1977); *Studia Biophys.*, **57**, 211–222 (1976).  
 (12) G. Lancelot, *Biochimie*, **59**, 587–596 (1977).  
 (13) G. Lancelot, *J. Am. Chem. Soc.*, **99**, 7037–7042 (1977).  
 (14) G. Lancelot and C. Hélène, *Proc. Natl. Acad. Sci. U.S.A.*, **74**, 4872–4875 (1977).  
 (15) D. R. Davies, *Annu. Rev. Biochem.*, **36**, 321–364 (1967).  
 (16) V. T. Ivanov, M. P. Filatova, Z. Reissman, T. O. Revtova, E. S. Efremov, V. S. Pashkov, S. G. Galaktionov, G. L. Grigoryan, and Yu. A. Ovchinnikov, "Structure-Biology", R. Walter and J. Meienhafer, Ed., Ann Arbor Science Publishers, Ann Arbor, Mich., 1975, pp 151–157.  
 (17) M. S. Lehmann, J. J. Verbist, W. C. Hamilton, and T. F. Koetzle, *J. Chem. Soc., Perkin Trans. 2*, 133–137 (1973).  
 (18) T. N. Bhat and M. Vijayan, *Acta Crystallogr., Sect. B*, **33**, 1754–1759 (1977).  
 (19) E. Wunsch and A. Zwick, *Chem. Ber.*, **97**, 3312–3316 (1964).  
 (20) L. Zervas, D. Borovas, and E. Gazis, *J. Am. Chem. Soc.*, **85**, 3360–3366 (1963).  
 (21) J. C. Howard, A. Ali, H. A. Scheraga, and F. A. Momany, *Macromolecules*, **8**, 607–622 (1975).  
 (22) C. H. Chang and L. G. Marzilli, *J. Am. Chem. Soc.*, **96**, 3656–3657 (1974).  
 (23) A. Bundi, C. Grathwohl, J. Hochmann, R. M. Keller, G. Wagner, and K. Wüthrich, *J. Magn. Reson.*, **18**, 191–198 (1975).  
 (24) M. Goodman, A. S. Verdini, C. Toniolo, W. D. Phillips, and F. A. Bovey, *Proc. Natl. Acad. Sci. U.S.A.*, **64**, 444–450 (1969).  
 (25) E. S. Pysh and C. Toniolo, *J. Am. Chem. Soc.*, **99**, 6211–6219 (1977).  
 (26) P. Keim, R. A. Vigna, J. S. Morrow, R. C. Marshall, and F. R. N. Gurd, *J. Biol. Chem.*, **248**, 7811–7818 (1973).  
 (27) C. Grathwohl and K. Wüthrich, *J. Magn. Reson.*, **13**, 217–225 (1974).  
 (28) B. N. Ramachandran, R. Chandrasekaran, and K. D. Kopple, *Biopolymers*, **10**, 2113–2131 (1971).  
 (29) R. A. Newmark and C. R. Cantor, *J. Am. Chem. Soc.*, **90**, 5010–5017 (1968).  
 (30) G. Lancelot, unpublished results.

## Comparison of Half-Met and Met Apo Hemocyanin. Ligand Bridging at the Binuclear Copper Active Site

Richard S. Himmelwright, Nancy C. Eickman, and Edward I. Solomon\*

Contribution from the Department of Chemistry, Massachusetts Institute of Technology, Cambridge, Massachusetts 02139. Received September 7, 1978

**Abstract:** Two series of *Busycon canaliculatum* hemocyanin derivatives have been prepared which have allowed a systematic study of ligand binding to the binuclear copper active site. Half-met-L hemocyanin, where L = CN<sup>-</sup>, NO<sub>2</sub><sup>-</sup>, N<sub>3</sub><sup>-</sup>, SCN<sup>-</sup>, OCN<sup>-</sup>, F<sup>-</sup>, Cl<sup>-</sup>, Br<sup>-</sup>, I<sup>-</sup>, CH<sub>3</sub>CO<sub>2</sub><sup>-</sup>, and aquo contains a [Cu(II)---Cu(I)] active site; for the met apo-L form, however, one copper has been selectively removed and the remaining copper oxidized, producing a [Cu(II)---( )] active site. A comparison of the ligand substitution chemistry of these forms has led to two general observations. First, ligands bind far more tightly to the half-met active site. This, combined with spectroscopic data and the effects of CO coordination, requires the exogenous ligand to bridge the coppers. Second, an additional coordination position is shown to be available at the Cu(II) site for only certain half-met-L forms (L = CN<sup>-</sup>, N<sub>3</sub><sup>-</sup>, SCN<sup>-</sup>), where the ligand is expected to keep the coppers >5 Å apart. No second coordination position is observed for any met apo derivative. These observations strongly support the presence of an endogenous protein bridge between the coppers. Furthermore, spectroscopic results have shown that certain half-met-L forms (L = Cl<sup>-</sup>, Br<sup>-</sup>, I<sup>-</sup>, N<sub>3</sub><sup>-</sup>) exhibit class II mixed valence properties (intervalence-transfer transitions and delocalized EPR) which directly correlate with the nature of the bridging ligand. Finally, half-met-L's, where L = N<sub>3</sub><sup>-</sup>, Cl<sup>-</sup>, CH<sub>3</sub>CO<sub>2</sub><sup>-</sup>, and aquo, are found to undergo reversible CO reactions which perturb the binding of L to the half-met active site.

Hemocyanin is a metalloprotein found in molluscs and arthropods which binds one oxygen molecule per binuclear copper active site.<sup>1</sup> The spectral features associated with the oxyhemocyanin active site are quite unusual as compared to known inorganic copper complexes.<sup>2</sup> In particular, while the copper is believed to be divalent, no EPR signal can be observed. This is generally ascribed to a reasonably strong magnetic coupling between the coppers, and susceptibility studies using the high sensitivity of a superconducting magnetometer have allowed a lower limit to be placed on antiferromagnetic exchange interaction of 550 cm<sup>-1</sup> based on the lack of a detectable signal.<sup>3</sup> The optical spectral properties of oxyhemocyanin are also unusual, with an intense band at 350 nm ( $\epsilon \sim 20\,000\text{ M}^{-1}\text{ cm}^{-1}$  per binuclear active site) and a reasonably intense transition at 570 nm ( $\epsilon \sim 1000\text{ M}^{-1}\text{ cm}^{-1}$ ) dominating the visible-UV spectral region.<sup>4</sup> Resonance Raman studies<sup>5</sup> into the visible absorption band allowed the O–O stretch to be observed at 749 cm<sup>-1</sup>, a value in the lower range of peroxide complexes,<sup>6</sup> and suggested that the oxygen atoms were equivalent in oxyhemocyanin. However, the mode of coordination of the peroxide to the binuclear copper site and the possibility of a protein residue bridging the two coppers have not been spectroscopically determined. These unique spectral properties make this protein an extremely interesting but difficult system to study in detail.

Several valid regenerable derivatives of this metalloprotein

have been prepared by different chemical routes. The met form of the protein (2Cu(II)) has been prepared by the action of peroxide on deoxyhemocyanin (2Cu(I))<sup>7</sup> or by artificial aging of oxy in excess ligand (N<sub>3</sub><sup>-</sup>, F<sup>-</sup>).<sup>8</sup> Like oxy-, methemocyanin is EPR-nondetectable,<sup>9,10</sup> the small EPR signal reported<sup>11,12</sup> for this form being associated with a damaged active site (~5%), resulting from the met preparation.<sup>9</sup> Alternatively, reacting deoxyhemocyanin with NO produces dimer hemocyanin which exhibits a large dipolar coupled EPR signal (the two Cu(II)'s in dimer are ~6 Å apart, based on computer simulation of the EPR signal<sup>13,14</sup>). Met and dimer hemocyanin can be interconverted and their optical spectral properties are quite similar, demonstrating that the interactions between the coppers leading to the large differences in ground-state EPR spectra are antiferromagnetic in nature.<sup>9</sup> The dimer preparation also shows an EPR signal associated with a single cupric site.<sup>13</sup> This could be obtained exclusively in large yield by the action of NaNO<sub>2</sub> at acid pHs on deoxyhemocyanin. In a preliminary communication,<sup>15</sup> we reported that this form undergoes complicated ligand substitution chemistry permitting a half-met-L [Cu(I)---Cu(II)L] series to be generated. Finally, we have shown<sup>16</sup> that for mollusc but not arthropod hemocyanin, one copper can be selectively removed from the active site and the remaining copper oxidized by a variety of small molecule oxidizing agents producing the met apo [Cu(II)---( )] derivative.

The mode of ligand binding to the binuclear copper active site is important in understanding the function of mollusc hemocyanin relative to other binuclear copper metalloproteins. The half-met form of the protein provides an appropriate system for the study of ligand coordination as the two coppers are completely different spectroscopically. The cupric site is easily studied by EPR and optical spectroscopic methods. The cuprous site, while not directly accessible spectroscopically, can still be probed in detail through a comparison of its effects on the half-met relative to the analogous met apo derivatives. The syntheses developed for the half-met and met apo derivatives are described and their spectral properties presented. A comparison between these forms is then used to demonstrate a bridging mode for exogenous ligand binding to the binuclear copper site and to verify the presence of an endogenous protein bridge.<sup>17</sup>

### Experimental Section

Hemocyanin was obtained from the marine snail, *Busycon canaliculatum*, by ultracentrifugation.<sup>18</sup> The half-met-NO<sub>2</sub><sup>-</sup> was prepared by treatment of the oxyprotein (~1 mM) with NaNO<sub>2</sub> (tenfold excess) and ascorbic acid (tenfold excess) for 12 h in pH 6.3 phosphate buffer at room temperature.<sup>13</sup> Ligand substitution reactions were performed at 4 °C by dialysis against buffer solutions containing an appropriate excess of added ligand. CN<sup>-</sup> ligand substitution was performed by adding excess CN<sup>-</sup> to a given half-met-L derivative followed by dialysis at pH 8.2 Tris buffer. The carbon-13 labeled NaCN was obtained at 90% enrichment from Kor Isotopes. Reduction of the half-met to regenerate oxyhemocyanin was performed with a freshly prepared Na<sub>2</sub>S<sub>2</sub>O<sub>4</sub> solution (~50 mM) under nitrogen to prevent decomposition. The reactions of the half-met with CO were carried out using a high-pressure reaction vessel. The dialysis experiments done under CO pressure were accomplished in a larger pressure apparatus (250 mL), with the dialysis tubing (containing 1 mL of half-met) placed in the buffer solution with one end left open above the dialysate level to allow for equilibrium with the CO atmosphere.

The copper content of the hemocyanin was monitored by atomic absorption using a Perkin-Elmer 360 spectrometer (equipped with a graphite furnace) in the preparation of the half-apo derivative [Cu(L)]<sub>2</sub>. Infusion of NaO<sub>2</sub> into a half-apo protein solution at pH 8.5 Tris was accomplished by a rapid injection of a saturated dimethylformamide (DMF) solution of NaO<sub>2</sub> from a hypodermic syringe. DMF in low concentrations had no effect on the protein. Regeneration of oxyhemocyanin from met apo was accomplished by adding a fivefold excess of Cu(CH<sub>3</sub>CN)<sub>4</sub>ClO<sub>4</sub> in 1 M acetonitrile under nitrogen.<sup>19</sup>

All EPR spectra were obtained from frozen solutions (0.5–1 mM protein) at 77 K using a liquid nitrogen Dewar or at temperatures >120 K using a liquid nitrogen cooled dry nitrogen flow system. A Varian E-9 EPR spectrometer was used operating at 9.1 GHz, 100-kHz modulation frequency and 20 G modulation amplitude. Protein derivatives for optical spectra were prepared by dialysis of the samples for ~12 h to a 1:1 (volume) sucrose:buffer solution at room temperature. The extremely viscous protein was then squeezed between two gasket-sealed quartz disks. EPR spectra of optical samples were checked prior to obtaining the optical spectra. Temperature-dependent spectra were obtained using a Cary 17 spectrometer and a Spectrim 11 cryocooler. Spectra taken in the IR region (1–2 μm) required the use of D<sub>2</sub>O, deuterated buffer, and deuterated sucrose to shift interfering water vibrations to lower energy. The difference spectra presented for the half-met-N<sub>3</sub><sup>-</sup> derivatives were taken relative to half-met-CH<sub>3</sub>CO<sub>2</sub><sup>-</sup>, a nonchromophoric ligand in this region.

### Results

**A. Preparative.** The ligand substitution chemistry of the half-met form of *Busycon canaliculatum* hemocyanin has been developed and used to generate a series of half-met-L derivatives (L = CN<sup>-</sup>, NO<sub>2</sub><sup>-</sup>, N<sub>3</sub><sup>-</sup>, SCN<sup>-</sup>, F<sup>-</sup>, Cl<sup>-</sup>, Br<sup>-</sup>, I<sup>-</sup>, CH<sub>3</sub>CO<sub>2</sub><sup>-</sup>, aquo), which permit detailed spectroscopic study of the mollusc active site. The original form obtained by oxidation of deoxyhemocyanin with sodium nitrite contains coordinated NO<sub>2</sub><sup>-</sup><sup>15</sup> (the half-met-NO<sub>2</sub><sup>-</sup> derivative). This ligand can be readily displaced only by CN<sup>-</sup> or N<sub>3</sub><sup>-</sup>. When

half-met-NO<sub>2</sub><sup>-</sup> is treated with a 100-fold excess of NaCN, at pH 8.0, 0.1 M Tris buffer, the green half-met-NO<sub>2</sub><sup>-</sup> is converted into an intermediate yellow form after 10 min. The excess CN<sup>-</sup> must then be removed rapidly by dialysis to prevent reduction and concomitant metal removal. Removal of the excess cyanide results in a stable purple derivative. This half-met-CN<sup>-</sup> form is substitution inert, as demonstrated by our inability to replace the bound CN<sup>-</sup> using large excesses (>100×) of other ligands. A 100-fold excess of NaN<sub>3</sub>, when added to half-met-NO<sub>2</sub><sup>-</sup> at pH 5.7 acetate buffer or pH 6.3 phosphate buffer, yields a reddish brown protein after 12 h in which the coordinated NO<sub>2</sub><sup>-</sup> has been displaced by N<sub>3</sub><sup>-</sup>. This is indicated by the large change in both the EPR and optical spectra. The N<sub>3</sub><sup>-</sup> remains coordinated on prolonged dialysis (>100 h) to pH 6.3 phosphate buffer; however, on dialysis to 0.1 M acetate buffer the reddish-brown color is lost after 36 h. The corresponding changes in the EPR spectrum indicate that acetate has replaced azide and is bound as a ligand at the active site.

Prolonged dialysis (>72 h) of half-met-CH<sub>3</sub>CO<sub>2</sub><sup>-</sup> to pH 6.3 phosphate buffer results in a change in the EPR spectrum, indicating that acetate is less tightly bound than either NO<sub>2</sub><sup>-</sup> or N<sub>3</sub><sup>-</sup>. Thus, half-met-CH<sub>3</sub>CO<sub>2</sub><sup>-</sup> in pH 6.3 phosphate buffer provides a convenient form for the generation of other half-met derivatives. The form obtained on extensive dialysis of half-met-CH<sub>3</sub>CO<sub>2</sub><sup>-</sup>, which will be referred to as half-met-aquo, can be reconverted to half-met-CH<sub>3</sub>CO<sub>2</sub><sup>-</sup> by treatment with a large excess (1000×) of acetate; however, this half-met-aquo form requires further characterization to determine the nature of the coordinated ligand.

Reaction of the half-met-CH<sub>3</sub>CO<sub>2</sub><sup>-</sup> in pH 6.3 phosphate buffer with a 100-fold excess of KSCN, NaCl, NaBr, or KI for 24 h, followed by dialysis to remove excess ligand, results in new EPR spectra associated with these half-met-L forms. Treatment of half-met-CH<sub>3</sub>CO<sub>2</sub><sup>-</sup> with a 500-fold excess of NaF is required to effect a spectral change. Dialysis to remove excess F<sup>-</sup> yields the half-met-aquo form as the EPR spectrum obtained is identical with that obtained from long-term dialysis (>100 h) of the half-met-CH<sub>3</sub>CO<sub>2</sub><sup>-</sup>. This provides an efficient route for conversion to the half-met-aquo form. It should be noted that this half-met-aquo derivative is the only form that shows a pH dependence in the EPR spectrum. Comparison of the previous ligand competition reactions produces the following trend in stability of the half-met-L forms: CN<sup>-</sup> >> NO<sub>2</sub><sup>-</sup> > N<sub>3</sub><sup>-</sup> > I<sup>-</sup> ~ Br<sup>-</sup> > SCN<sup>-</sup> ~ Cl<sup>-</sup> > CH<sub>3</sub>CO<sub>2</sub><sup>-</sup> >> F<sup>-</sup>.

Oxyhemocyanin can be regenerated from the half-met form of the protein by one-electron reduction followed by exposure to oxygen. Derivatives which contain more weakly coordinated ligands such as CH<sub>3</sub>CO<sub>2</sub><sup>-</sup> are readily reduced with a tenfold excess of Na<sub>2</sub>S<sub>2</sub>O<sub>4</sub> (Figure 1). The reaction requires prior binding of the reducing agent as shown by the appearance of an intermediate EPR signal obtained from partially reduced samples, and by the inhibition of the regeneration by more stable ligands (CN<sup>-</sup> and NO<sub>2</sub><sup>-</sup>). Dialysis to remove the excess Na<sub>2</sub>S<sub>2</sub>O<sub>4</sub> followed by exposure of the protein to oxygen results in elimination of the EPR signal and essentially complete recovery of the 345-nm absorption band associated with the oxy form. Ascorbic acid and outer sphere reducing agents are found to be ineffective in reduction of the half-met-CH<sub>3</sub>CO<sub>2</sub><sup>-</sup> form, while hydroxylamine<sup>20</sup> requires large excesses and long reaction times for reduction of the half-met-NO<sub>2</sub><sup>-</sup> form. The half-met substitution chemistry is summarized in Scheme 1.

Certain half-met-L derivatives have the ability to coordinate more than one exogenous ligand. Treatment of half-met-CN<sup>-</sup>, -N<sub>3</sub><sup>-</sup>, and -SCN<sup>-</sup> with a 100-fold excess of CN<sup>-</sup>, N<sub>3</sub><sup>-</sup>, and SCN<sup>-</sup>, respectively, produces large changes in both the EPR and optical spectra of these forms (see next section on spectroscopic results). No other half-met derivatives show this

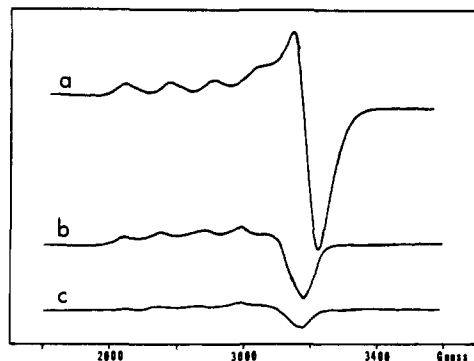
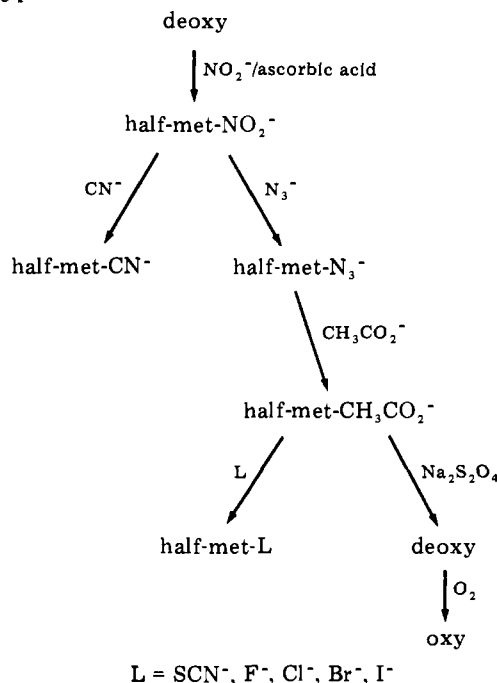


**Figure 1.** Change in the EPR spectrum of half-met- $\text{CH}_3\text{CO}_2^-$  upon reduction with tenfold excess  $\text{Na}_2\text{S}_2\text{O}_4$ : (a) half-met- $\text{CH}_3\text{CO}_2^-$ , pH 6.3 phosphate buffer, 77 K; (b) after 30 min  $\text{Na}_2\text{S}_2\text{O}_4$ ; (c) after 60 min  $\text{Na}_2\text{S}_2\text{O}_4$ .

#### Scheme I



behavior. Coordination of a second ligand, different from the first, could only be considered for half-met- $\text{CN}^-$ , as for other half-met-L forms, L is replaced when an excess of different ligand is added. The EPR spectrum (see Table I) and color (purple  $\rightarrow$  gold) of half-met- $\text{CN}^-$  are found to change in the presence of 100-fold excess  $\text{N}_3^-$ , indicating that an  $\text{N}_3^-$  is bound in addition to the original  $\text{CN}^-$ . Upon dialysis for 24 h to pH 6.3 phosphate, the half-met- $\text{CN}^-$  EPR spectrum is completely recovered. No other ligands were found to produce observable spectral changes when added in excess to half-met- $\text{CN}^-$ .

A number of the half-met derivatives ( $\text{Cl}^-$ ,  $\text{CH}_3\text{CO}_2^-$ ,  $\text{N}_3^-$ , aquo) undergo a reversible reaction with carbon monoxide. When half-met- $\text{Cl}^-$ , - $\text{CH}_3\text{CO}_2^-$ , and -aquo are treated with CO at 30 psi in pH 6.3 phosphate buffer for 30 min a large change in EPR spectrum is observed. Repeated evacuation followed by flushing with  $\text{N}_2$  results in recovery of the original EPR spectrum. Half-met- $\text{N}_3^-$ , as well as half-met- $\text{N}_3^-$  in the presence of excess  $\text{N}_3^-$ , also shows a reversible reaction with CO, the CO adduct being stable for approximately 2 h after removal of the CO pressure. Half-met-L, where L =  $\text{CN}^-$ ,  $\text{NO}_2^-$ ,  $\text{SCN}^-$ ,  $\text{Br}^-$ , and  $\text{I}^-$ , show no observable CO reaction when treated with CO at higher pressures (up to 50 psi) for longer reaction times (>12 h).

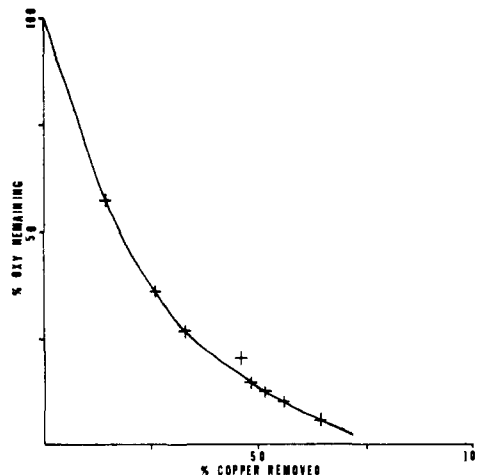


**Figure 2.** Plot of oxygen binding as a function of amount of copper removed from *Busycon canaliculatum* hemocyanin upon treatment with cyanide.

**Table I.** Half-Met-L EPR Parameters

half-met-L L =	$g_{\parallel}$	$g_{\perp}$	$A_{\parallel}$ , $10^{-4} \text{ cm}^{-1}$
$\text{N}_3^-$ , 220 K	2.277	2.082	108
$\text{N}_3^-$ , + CO	2.219	2.052	176
excess $\text{N}_3^-$	2.242	2.062	136
excess $\text{N}_3^-$ , + CO	2.213	2.041	170
$\text{SCN}^-$	2.275	2.060	170
excess $\text{SCN}^-$	2.251	2.064	179
$\text{CN}^-$	2.291	2.069	150
excess $\text{CN}^-$	2.239	2.057	174
$\text{CN}^-$ , excess $\text{N}_3^-$	2.257	2.054	158
$\text{NO}_2^-$	2.302	2.096	125
$\text{C}_2\text{H}_3\text{O}_2^-$	2.318	2.080	141

Treatment of deoxyhemocyanin with  $\text{CN}^-$  is the general method used to remove all the copper from the holoprotein.<sup>21</sup> However, when *Busycon canaliculatum* hemocyanin was treated with 0.05 M NaCN at pH 8.2, 0.1 M Tris in the presence of 0.1 M  $\text{CaCl}_2$  for 12.5 h, one copper was found to be selectively removed from each active site. Figure 2 plots the percent of oxyhemocyanin present for protein samples from which various amounts of copper have been removed. The percent of oxyhemocyanin present is given by the absorption at 345 nm relative to the 280-nm protein absorption obtained after removal of  $\text{CN}^-$  and exposure to oxygen. Thus, when about 50% of the copper has been removed, all of the oxygen binding ability has been eliminated. Since oxyhemocyanin has been shown to bind one oxygen molecule per 2 Cu, this requires that one Cu(I) remain per active site in the half-apo protein.

This half-apo form can then be oxidized via a number of routes using small molecule oxidizing agents. When the half-apo protein is incubated with a 20-fold excess of  $\text{NaNO}_2$  at pH 6.3 phosphate buffer for 36 h, the copper is oxidized to the 2+ oxidation state, as shown by the appearance of a cupric EPR spectrum. No change in the intensity of this spectrum was observed upon extensive dialysis, demonstrating that the Cu(II) remains tightly bound to the protein, and double integration of the EPR signal indicates that it accounts for 50% of the available sites (as determined by absorption at 280 nm). The half-apo protein derivatives can also be oxidized by performing a superoxide infusion reaction at basic pHs to avoid disproportionation of  $\text{O}_2^-$  in aqueous solution. The met apo obtained by oxidation with  $\text{NaNO}_2$  and dialyzed to pH 8.5,

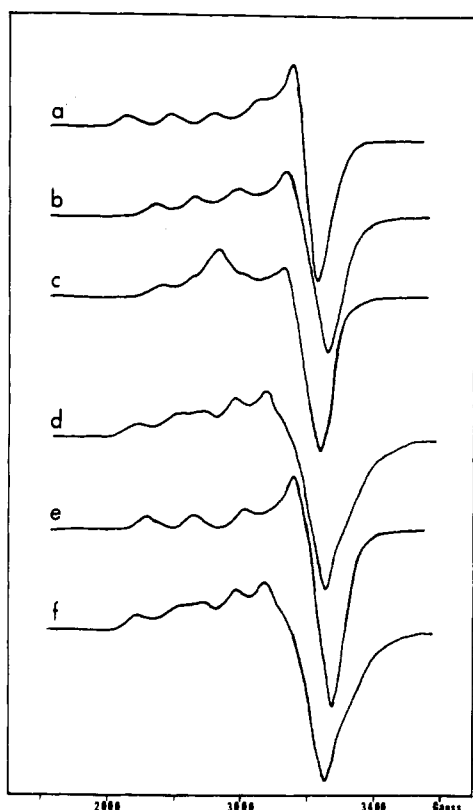


**Figure 3.** EPR comparison of the ligand substitution chemistry of half-met and met apo hemocyanin: (a) half-met- $\text{CH}_3\text{CO}_2^-$  in pH 6.3 phosphate buffer; (b) half-met- $\text{CH}_3\text{CO}_2^-$  + 100-fold excess  $\text{N}_3^-$ ; (c) dialysis of b for 100 h against pH 6.3 phosphate buffer; (d) met apo-aquo in pH 6.3 phosphate buffer; (e) met apo-aquo + 100-fold excess  $\text{N}_3^-$ ; (f) dialysis of e for 24 h against pH 6.3 phosphate buffer. Spectra recorded at 77 K.

0.1 M Tris buffer exhibits an EPR spectrum identical with that of the  $\text{NaO}_2$  oxidation product. The half-apo can also be partially oxidized by incubation at 37 °C for 36 h at pH 6.3 phosphate buffer in a similar manner to artificial aging<sup>8</sup> of native hemocyanin. This method, however, generally produces a lower, more variable conversion. Treatment of the half-apo protein with a 50-fold excess of hydrogen peroxide at pH 8.5, 0.1 M Tris buffer also results in the appearance of an EPR spectrum. The EPR spectrum obtained in this reaction differs from that of previous preparations and the copper(II) is found to be easily removed by dialysis. Attempts to oxidize the half-apo protein with  $\text{Fe}(\text{OH})_2^{3+}$  and  $\text{Fe}(\text{CN})_6^{3-}$  proved unsuccessful.

This met apo derivative, containing a  $[\text{Cu}(\text{II})\cdots(\quad)]$  active site, readily undergoes ligand substitution reactions. Dialysis to remove excess nitrite from the met apo produced in the nitrite preparation results in a large change in the EPR spectrum indicating replacement of  $\text{NO}_2^-$  with a water ligand (phosphate buffer) or an acetate ligand (acetate buffer). Ligand substitution results for either met apo form when treated with a 100-fold excess of  $\text{N}_3^-$ ,  $\text{NO}_2^-$ ,  $\text{CH}_3\text{CO}_2^-$ , or  $\text{SCN}^-$ . Treatment of met apo-aquo with a tenfold excess of  $\text{CN}^-$  at pH 7.6 phosphate buffer produces a stable  $\text{CN}^-$  derivative. If  $\text{CN}^-$  is added in larger excess or at higher pH, however, reduction rapidly takes place. The halide ions must be present in large excess (500 $\times$ ) to achieve a reasonable conversion to the met apo-halide forms. These ligand competition reactions produce the following general series for the stability of the met apo-L forms:  $\text{CN}^- \sim \text{N}_3^- \sim \text{SCN}^- > \text{NO}_2^- \sim \text{CH}_3\text{CO}_2^- > \text{aquo} > \text{halides}$ .

A comparison of the ligand substitution reactivity of the half-met-L and met apo-L series leads to the generalization

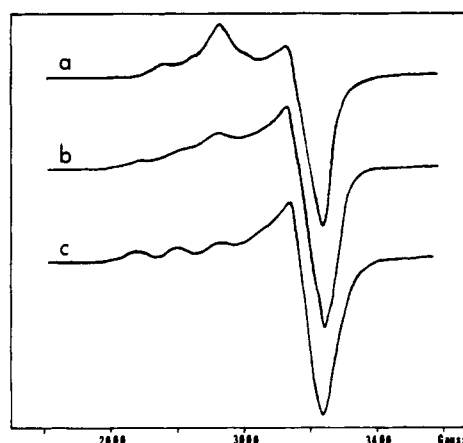


**Figure 4.** Effects on the half-met- $\text{N}_3^-$  EPR spectrum of dialysis against pH 6.3 phosphate buffer under CO pressure: (a) half-met- $\text{N}_3^-$  in pH 6.3 phosphate buffer, 77 K; (b) a after 12-h dialysis under 30 psi of CO; (c) a after 28-h dialysis under 30 psi of CO.

that for all cases the ligands are much more tightly bound to the half-met than the met apo forms of the protein. This is well illustrated by considering the ligand substitution chemistry of parallel forms. Preparation of half-met- $\text{CH}_3\text{CO}_2^-$  and met apo- $\text{CH}_3\text{CO}_2^-$  followed by dialysis against pH 6.3 phosphate buffer for 24 h yields the half-met- $\text{CH}_3\text{CO}_2^-$  and met apo-aquo forms whose spectra are shown in Figures 3a and 3d. The effects of treating these forms with a 100-fold excess of  $\text{N}_3^-$  are then shown in Figures 3b and 3e. After dialysis of the half-met- $\text{N}_3^-$  (in 100 $\times$  excess  $\text{N}_3^-$ ) for 100 h against pH 6.3 phosphate buffer, the EPR spectrum remaining (Figure 3c) differs from a and b and is associated with a bound  $\text{N}_3^-$ . However, dialysis of the met apo- $\text{N}_3^-$  (in 100 $\times$  excess  $\text{N}_3^-$ ) for only 24 h at pH 6.3 phosphate results in complete recovery of the met apo-aquo spectrum (Figure 3f). A qualitative estimate of the relative ligand binding strengths for a number of half-met-L and met apo-L forms can be obtained from the dialysis times (against pH 6.3 phosphate buffer) required for complete conversion to the aquo forms. Half-met-L derivatives, where  $\text{L} = \text{CN}^-$ ,  $\text{NO}_2^-$ ,  $\text{N}_3^-$ ,  $\text{SCN}^-$ ,  $\text{Cl}^-$ ,  $\text{Br}^-$ , and  $\text{I}^-$ , show no conversion to half-met-aquo upon dialysis for >100 h. Half-met- $\text{CH}_3\text{CO}_2^-$  shows significant conversion (~20%) to the half-met-aquo form after 72 h of dialysis and  $\text{F}^-$  is eliminated from half-met- $\text{F}^-$  within 24 h of dialysis. In contrast, the met apo-L forms, where  $\text{L} = \text{CN}^-$ ,  $\text{NO}_2^-$ ,  $\text{N}_3^-$ ,  $\text{SCN}^-$ ,  $\text{Cl}^-$ ,  $\text{Br}^-$ ,  $\text{I}^-$ , and  $\text{CH}_3\text{CO}_2^-$ , are converted to met apo-aquo within 24 h upon dialysis and the  $\text{F}^-$  is not observed to coordinate even in 500 $\times$  excess  $\text{F}^-$ .

Figure 4 presents the spectrum of half-met- $\text{N}_3^-$  after 12 and 28 h of dialysis under 30-psi CO pressure after removal of the CO by evacuation and flushing with nitrogen. Thus, although the azide cannot be removed from the half-met- $\text{N}_3^-$  by dialysis alone, dialysis under 30 psi of CO results in complete conversion to the half-met-aquo form after 28 h. Similar experiments were carried out for half-met- $\text{Cl}^-$  and half-met- $\text{CH}_3\text{CO}_2^-$ . Dialysis of half-met- $\text{CH}_3\text{CO}_2^-$  under 30 psi of CO increased the rate of acetate removal when compared to dialysis with no CO pressure against pH 6.3 phosphate buffer. However, chloride remained coordinated in half-met- $\text{Cl}^-$  after dialysis under 30-psi CO pressure for 36 h.

**B. Spectroscopic.** Certain spectroscopic properties are particularly useful for each type of ligand in determining the nature of the ligand binding to the active site in the half-met-L (and met apo-L) derivatives. Appropriate spectral regions are presented below by class of ligands studied.

**1. Pseudohalide Derivatives.** Figure 5 presents the EPR spectra associated with various chemical perturbations on the

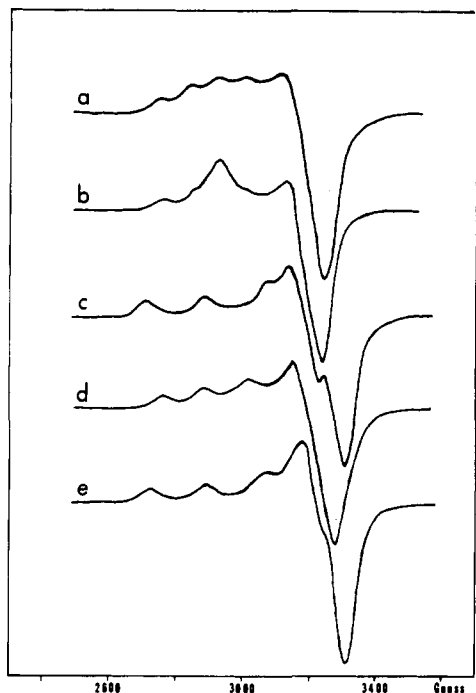


Figure 5. Effects of perturbations on the half-met- $\text{N}_3^-$  EPR spectrum (in pH 6.3 phosphate buffer): (a) half-met- $\text{N}_3^-$  at 220 K; (b) half-met- $\text{N}_3^-$  at 77 K; (c) half-met- $\text{N}_3^- + \text{CO}$ ; (d) half-met- $\text{N}_3^- + 100\text{-fold excess } \text{N}_3^-$ ; (e) d + CO (c-e recorded at 77 K).

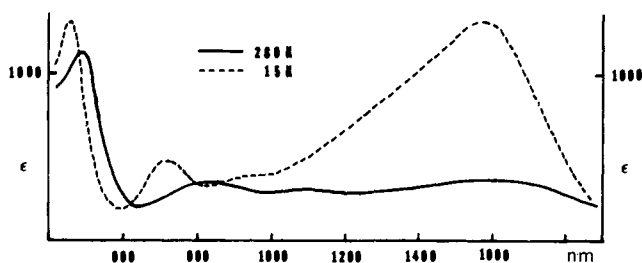


Figure 6. Temperature dependence of the absorption spectrum of half-met- $\text{N}_3^-$  (in pH 6.3 phosphate buffered sucrose glasses).

half-met- $\text{N}_3^-$  derivative. The optical spectra in the visible and near-IR region (400 nm–2  $\mu\text{m}$ ) associated with half-met- $\text{N}_3^-$  are presented in Figure 6. The effects of chemical perturbations on the charge-transfer (CT) region (400–500 nm) are given as difference spectra in Figure 7. Figure 7 also includes a met apo spectrum for comparison.

Half-met- $\text{N}_3^-$  at temperatures above 200 K exhibits a normal axial copper(II) EPR spectrum with a rather small parallel hyperfine splitting (see Table I for all half-met-L EPR parameters). This form exhibits d-d transitions at 800 nm ( $\epsilon \sim 200 \text{ M}^{-1} \text{ cm}^{-1}$ ) in its absorption spectrum and a charge-transfer transition at 490 nm ( $\epsilon \sim 1000 \text{ M}^{-1} \text{ cm}^{-1}$ ). Upon lowering the temperature, the EPR spectrum of the half-met- $\text{N}_3^-$  is found to drastically change into the unique spectrum shown in Figure 5b. This temperature effect is associated with a large increase in energy of the d-d and charge-transfer transitions and the appearance of a new spectral feature in the near IR ( $\lambda_{\text{max}} 1550 \text{ nm}$ ;  $\epsilon \sim 1200 \text{ M}^{-1} \text{ cm}^{-1}$ ). Addition of excess azide is found to eliminate this temperature effect and produce an additional more intense charge-transfer transition at higher energy ( $\lambda_{\text{max}} 410 \text{ nm}$ ,  $\epsilon \sim 1500 \text{ M}^{-1} \text{ cm}^{-1}$ ). Carbon monoxide has a large effect on the EPR spectra of the half-met- $\text{N}_3^-$  and half-met- $\text{N}_3^-$  in excess  $\text{N}_3^-$  and produces small optical spectral changes. Shifts in the CT region are difficult to estimate accurately as the CO also affects the residual oxy

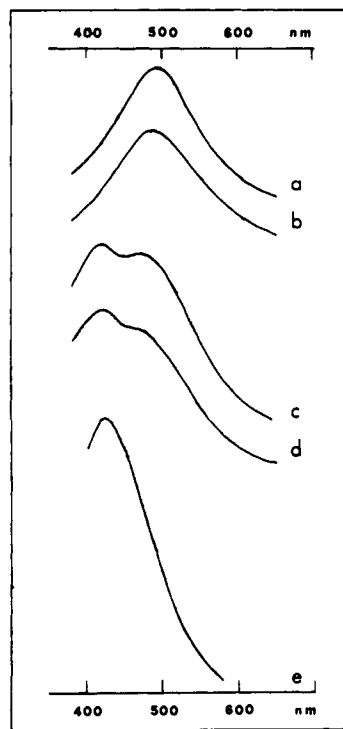


Figure 7. Effects of perturbations on the charge-transfer spectrum of half-met- $\text{N}_3^-$  (in pH 6.3 phosphate buffer, 293 K): (a) half-met- $\text{N}_3^-$ ; (b) half-met- $\text{N}_3^- + \text{CO}$ ; (c) half-met- $\text{N}_3^-$  in excess  $\text{N}_3^-$ ; (d) half-met- $\text{N}_3^-$  in excess  $\text{N}_3^- + \text{CO}$ ; (e) met apo- $\text{N}_3^-$ . Spectra were taken with half-met- $\text{CH}_3\text{CO}_2^-$  (for a, b, c, and d) or met apo-aquo (for e) in the reference beam.  $\epsilon$ 's are given in the text.

Table II. Met Apo-L EPR Parameters

met apo-L L =	$g_{\parallel}$	$g_{\perp}$	$A_{\parallel}$ , $10^{-4} \text{ cm}^{-1}$
$\text{N}_3^-$	2.240	2.058	152
$\text{SCN}^-$	2.264	2.055	169
$\text{CN}^-$	2.275	2.067	128
$\text{Cl}^-$	2.248	2.074	168
$\text{Br}^-$	2.245	2.065	162
$\text{I}^-$	2.233	2.058	167

present in these derivatives; however, the CT transition at 490 nm is observed qualitatively to shift up in energy by  $\sim 10 \text{ nm}$ . The met apo- $\text{N}_3^-$  form exhibits a normal copper(II) EPR spectrum (see Table II for met apo-L EPR parameters), ligand field transitions at 710 nm ( $\epsilon \sim 200 \text{ M}^{-1} \text{ cm}^{-1}$ ), and a CT transition at 420 nm ( $\epsilon \sim 2500 \text{ M}^{-1} \text{ cm}^{-1}$ ).

The EPR spectra of the half-met- $\text{SCN}^-$ , half-met- $\text{SCN}^-$  in excess  $\text{SCN}^-$ , and met apo- $\text{SCN}^-$  are given in Figure 8. The visible and near-UV spectral regions of these forms are given in Figure 9. Unfortunately the optical spectrum of the half-met- $\text{SCN}^-$  form is complicated by the fact that the preparation requires dialysis to excess  $\text{SCN}^-$ . The high concentration ( $\sim 0.1 \text{ M}$ ) of KSCN yields reduction of some (5–10%) half-met sites, which upon removal of excess  $\text{SCN}^-$  become oxygenated, resulting in overlap by the intense oxy spectral features in this region. While the oxy features obscure the CT region of half-met- $\text{SCN}^-$ , the ligand field transitions are observed at approximately 700 nm and no spectral features are observed in the near-IR region. Addition of excess  $\text{SCN}^-$  yields d-d transitions at  $\sim 800 \text{ nm}$  ( $\epsilon \sim 200 \text{ M}^{-1} \text{ cm}^{-1}$ ) and weak CT transitions ( $\epsilon < 300 \text{ M}^{-1} \text{ cm}^{-1}$ ) are observed in the 400–600-nm region. The met apo- $\text{SCN}^-$  has ligand field transitions

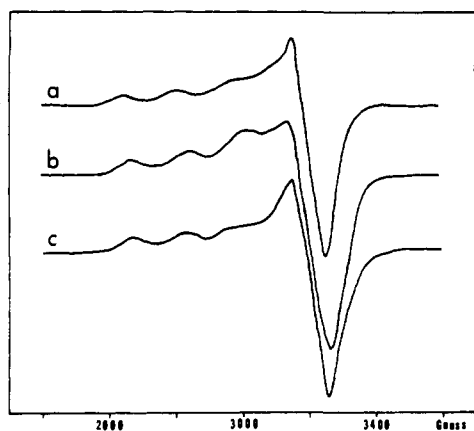


Figure 8. EPR spectra of  $\text{SCN}^-$  derivatives (in pH 6.3 phosphate buffer, 77 K): (a) half-met- $\text{SCN}^-$ ; (b) half-met- $\text{SCN}^-$  + 100-fold excess  $\text{SCN}^-$ ; and (c) met apo- $\text{SCN}^-$  in 100-fold excess  $\text{SCN}^-$ .

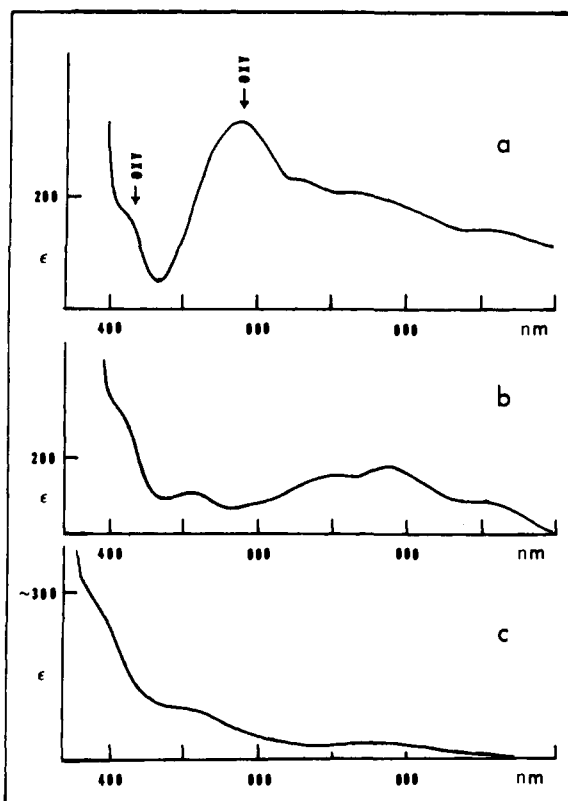


Figure 9. Absorption spectra of  $\text{SCN}^-$  derivatives (in pH 6.3 phosphate buffered sucrose glasses, 15 K): (a) half-met- $\text{SCN}^-$  (absorption due to contaminating oxyhemocyanin is indicated by arrows); (b) half-met- $\text{SCN}^-$  in excess  $\text{SCN}^-$ ; (c) met apo- $\text{SCN}^-$ .

at  $\sim 780$  nm and exhibits weak CT transitions at 410 and 540 nm ( $\epsilon < 300 \text{ M}^{-1} \text{ cm}^{-1}$ ).

**2. Cyanide Derivatives.** The EPR spectra of half-met- $\text{CN}^-$ , half-met- $\text{CN}^-$  in excess  $\text{CN}^-$ , and met apo- $\text{CN}^-$  are presented in Figure 10a,c,e. The  $g$  and  $A$  values are observed to be significantly affected by the addition of excess cyanide to the half-met- $\text{CN}^-$ . Associated with this behavior is a large shift in the d-d transitions to higher energy ( $\Delta\bar{\nu} = 3800 \text{ cm}^{-1}$ ).

The most effective probe of the mode of cyanide coordination on the copper(II) should be the superhyperfine broadening of the copper(II) parallel hyperfine lines due to carbon-13 labeling of cyanide.<sup>22</sup> These effects are presented in Figure 10b,d,f under each equivalent  $^{12}\text{C}^-$  EPR spectrum. Although

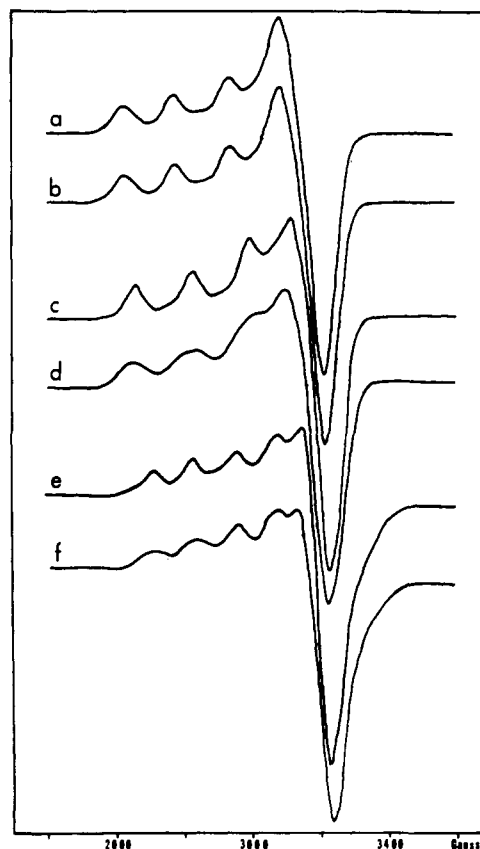


Figure 10. Effects of  $^{13}\text{C}$  labeling on the EPR spectra of half-met- $\text{CN}^-$  and met apo- $\text{CN}^-$  (in pH 8.0 Tris buffer, 77 K): (a) half-met- $\text{CN}^-$ ; (b) half-met- $^{13}\text{C}^-$ ; (c) half-met- $\text{CN}^-$  + 100-fold excess  $\text{CN}^-$ ; (d) half-met- $\text{CN}^-$  + 100-fold excess  $^{13}\text{C}^-$ ; (e) met apo- $\text{CN}^-$ ; and (f) met apo- $^{13}\text{C}^-$ .

the copper hyperfine lines associated with half-met- $^{12}\text{C}^-$  are already fairly broad, no further broadening is observed upon carbon-13 labeling for half-met- $\text{CN}^-$ . In strong contrast to this behavior, the half-met- $\text{CN}^-$  in excess  $^{13}\text{C}^-$  and the met apo- $^{13}\text{C}^-$  are observed to have significantly broadened parallel hyperfine features relative to their  $^{12}\text{C}^-$  analogues.

**3. Halide Derivatives.** The EPR spectra of the half-met-X series, where X =  $\text{F}^-$ ,  $\text{Cl}^-$ ,  $\text{Br}^-$ , and  $\text{I}^-$ , are presented in Figure 11. Unusual parallel hyperfine patterns are observed for these derivatives which are particularly evident in the  $\text{Br}^-$  and  $\text{I}^-$  forms (uneven, small  $A_{\parallel}$  splitting with more than four components). Investigation of the temperature dependence of these EPR spectra demonstrated that only the half-met- $\text{I}^-$  shows any change with temperature, the hyperfine lines becoming more well defined at low temperature (77 K). All the met apo-X derivatives show normal  $g$  values and hyperfine splittings in contrast to the half-met-X forms (see Table II). (Note that the EPR parameters of met apo- $\text{F}^-$  were not included since  $\text{F}^-$  was not found to bind even in 500-fold excess.)

The optical spectra of the half-met-X series are presented in Figure 12. The ligand field transitions of the half-met-X forms are found at 725 ( $\text{F}^-$ ), 670 ( $\text{Cl}^-$ ), 710 ( $\text{Br}^-$ ), and 740 nm ( $\text{I}^-$ ). In addition, a new spectral feature appears in the near-IR not present in met apo-X equivalents for half-met- $\text{Cl}^-$ ,  $\text{Br}^-$ , and  $\text{I}^-$ . This IR band increases in intensity over the series  $\text{Cl}^- < \text{Br}^- < \text{I}^-$  and decreases in energy with  $\text{Cl}^- > \text{Br}^- > \text{I}^-$  (energies and intensities are presented in Table III). Finally, only the half-met- $\text{I}^-$  exhibits weak low-energy charge-transfer transitions ( $\lambda$  430 nm,  $\epsilon \sim 500 \text{ M}^{-1} \text{ cm}^{-1}$ ;  $\lambda$  520 nm,  $\epsilon \sim 200 \text{ M}^{-1} \text{ cm}^{-1}$ ) in the visible spectral region.

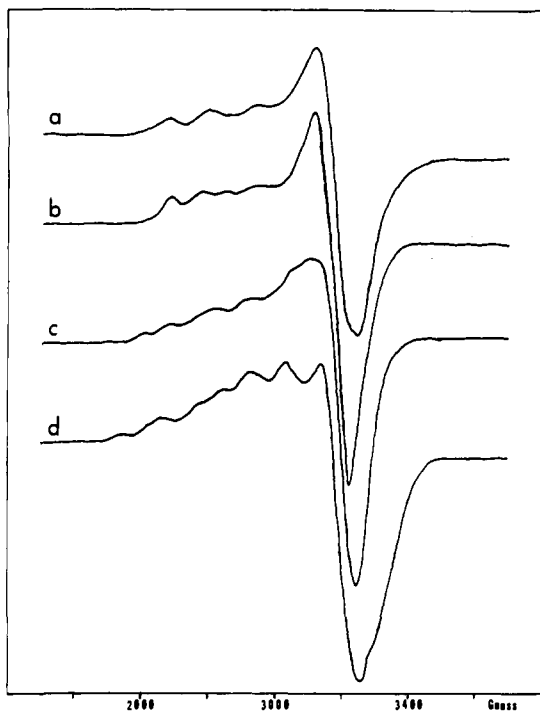


Figure 11. EPR spectra of half-met-halides (in pH 6.3 phosphate buffer, 77 K): (a) half-met-F<sup>-</sup> in 100-fold excess F<sup>-</sup>; (b) half-met-Cl<sup>-</sup>; (c) half-met-Br<sup>-</sup>; and (d) half-met-I<sup>-</sup>.

Table III. Energies and Intensities of the 1T Transitions of Half-Met-X Derivatives

X	$E_{\max}$ , cm <sup>-1</sup>	$\epsilon$ , M <sup>-1</sup> cm <sup>-1</sup>
Cl <sup>-</sup>	10 900	400
Br <sup>-</sup>	10 100	600
I <sup>-</sup>	8 400	1200

**4. Other Derivatives.** The EPR and optical spectra of half-met-NO<sub>2</sub><sup>-</sup> and half-met-CH<sub>3</sub>CO<sub>2</sub><sup>-</sup> are presented in Figures 13 and 14. Both exhibit normal cupric EPR parameters and ligand field transitions ( $\lambda_{\text{NO}_2^-}$  680 nm,  $\epsilon \sim 100 \text{ M}^{-1} \text{ cm}^{-1}$ ;  $\lambda_{\text{CH}_3\text{CO}_2^-}$  720 nm,  $\epsilon \sim 100 \text{ M}^{-1} \text{ cm}^{-1}$ ). No near-IR or charge-transfer spectral features are observed for either derivative. The EPR spectra of half-met-aquo and met-aquo<sup>23</sup> at pH 6.3 phosphate buffer are given in Figure 15a,b.

#### Discussion

The asymmetry of the [Cu(II)⋯Cu(I)] active site in the half-met derivatives provides a mechanism for directly differentiating the roles of the two coppers in exogenous ligand coordination. Further, a comparison of the cupric sites in the half-met-L [Cu(II)⋯Cu(I)] with the parallel met apo-L [Cu(II)⋯( )] form allows the effects of the Cu(I) on the Cu(II) to be determined. The results of our chemical and spectroscopic studies on half-met and met apo derivatives of *Busycon canaliculatum* hemocyanin have led to two major conclusions. *First, exogenous ligands are found to bridge the [Cu(II)⋯Cu(I)] half-met site, thus indicating a bridging geometry for peroxide in oxyhemocyanin.* Much larger ligand binding constants are associated with the half-met-L relative to the equivalent met apo-L form of the protein. This requires that the Cu(I) of the half-met site is involved in binding the exogenous ligand. Coordination at the Cu(I) is also supported by the effects of CO on these binding constants. It is most reasonable to expect CO to bind to the Cu(I) site. In the case

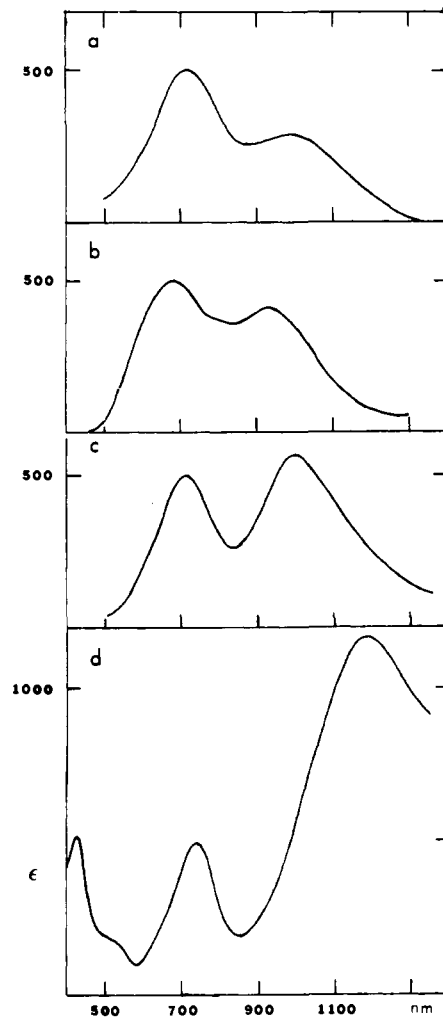


Figure 12. Absorption spectra of half-met-halides (in pH 6.3 phosphate buffered sucrose glasses, 15 K): (a) half-met-F<sup>-</sup>; (b) half-met-Cl<sup>-</sup>; (c) half-met-Br<sup>-</sup>; (d) half-met-I<sup>-</sup>.

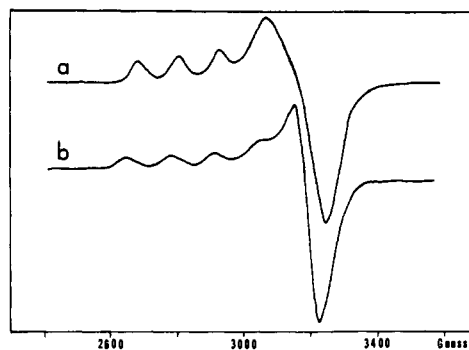


Figure 13. EPR spectra (in pH 6.3 phosphate buffer, 77 K) of (a) half-met-NO<sub>2</sub><sup>-</sup> and (b) half-met-CH<sub>3</sub>CO<sub>2</sub><sup>-</sup>.

of half-met-N<sub>3</sub><sup>-</sup>, coordination of the CO to the Cu(I) is found to greatly reduce the affinity of the half-met site for the N<sub>3</sub><sup>-</sup> to a level comparable to that of the met apo-N<sub>3</sub><sup>-</sup> form and consistent with Cu(II) substitution chemistry.<sup>24</sup> The high binding strengths associated with exogenous ligand coordination to the Cu(I) in half-met can be explained based on the known substitution chemistry of Cu(I) complexes<sup>25</sup> and their extremely low affinity for water as ligands. In fact, the high affinity of the binuclear cuprous site in deoxyhemocyanins for oxygen may be associated with this inability of the unsaturated

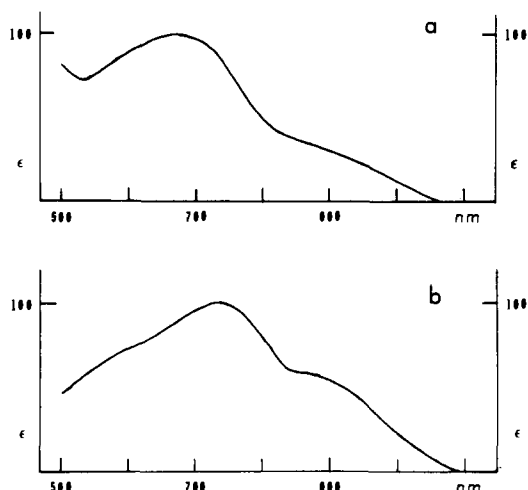


Figure 14. Absorption spectra (in pH 6.3 phosphate buffered sucrose glasses) of (a) half-met- $\text{NO}_2^-$  and (b) half-met- $\text{CH}_3\text{CO}_2^-$ .

Cu(I) site to aquate, thereby leaving an open coordination position on the Cu(I) for interaction with oxygen.

The spectral data associated with the cupric site in the half-met forms also demonstrate that the exogenous ligand is binding to the Cu(II). These data include large changes in the EPR and ligand field spectra with variations in L combined with the appearance of  $L \rightarrow M$  charge-transfer transitions (LMCT) for appropriate ligands. Thus, the exogenous ligand must be bridging the two coppers. Further confirmation of a bridging mode for L is provided by the appearance of intervalence-transfer (IT) transitions<sup>26</sup> for a number of half-met-L forms (vide supra). The fact that open coordination positions are present at both coppers in the half-met derivatives also strongly supports a bridging mode for peroxide in oxyhemocyanin and exogenous ligands bound to methemocyanin.

The second conclusion based on a comparison of the half-met and met apo forms of the protein is that there is an endogenous protein bridge between the two coppers. For all ligands studied, only one exogenous ligand is found to bind to the met apo Cu(II) site. In contrast, these ligands can be placed in two groups based on their ability to coordinate to the half-met site. For half-met- $L_1$  derivatives where  $L_1 = \text{CH}_3\text{CO}_2^-$ ,  $\text{NO}_2^-$ ,  $\text{F}^-$ ,  $\text{Cl}^-$ ,  $\text{Br}^-$ , and  $\text{I}^-$ , it is possible to bind only one exogenous ligand to the active site, whereas for half-met- $L_2$  derivatives, where  $L_2 = \text{CN}^-$ ,  $\text{N}_3^-$ , and  $\text{SCN}^-$ , a second ligand is found to coordinate in excess. For the half-met derivatives the discussion to follow uses the spectroscopic results for specific ligands to determine linkage isomerization and therefore estimate Cu(II)-Cu(I) distances for these derivatives. The  $L_1$  ligands are expected to keep the metals between 2.6 and 3.6 Å apart, distances which would also allow a protein bridge to be present. For  $L_2 = \text{CN}^-$ ,  $\text{N}_3^-$ , and  $\text{SCN}^-$ , however, these Cu(II)-Cu(I) distances are between 5.0 and 5.3 Å. The metals would then be too far apart to maintain a protein bridge. Rupture of the bridge would then leave a second coordination position available on the Cu(II). For met apo, the removal of the Cu(I) allows this protein ligand to coordinate more tightly to the Cu(II), blocking the second coordination position. Such a scheme (see Scheme II) would also provide an explanation for the large differences in magnetic interactions between the Cu(II)'s in oxy- and met- as compared to dimer hemocyanin. The binuclear cupric distance for oxyhemocyanin has been determined by EXAFS studies<sup>27</sup> to be  $\sim 3.6$  Å, while simulation of the EPR spectrum<sup>14</sup> of dimer hemocyanin has placed the metals at  $\sim 6$  Å separation for this derivative. The reaction of half-met- $\text{NO}_2^-$  with nitric oxide, oxidizing the second copper to produce dimer hemocyanin, may be associated with the

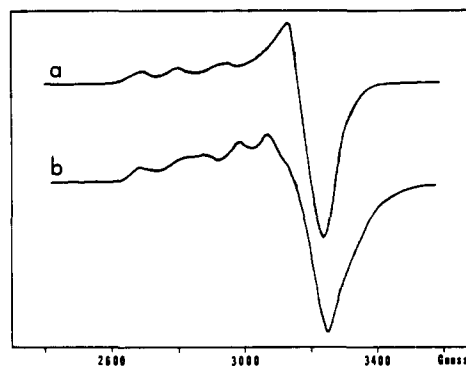
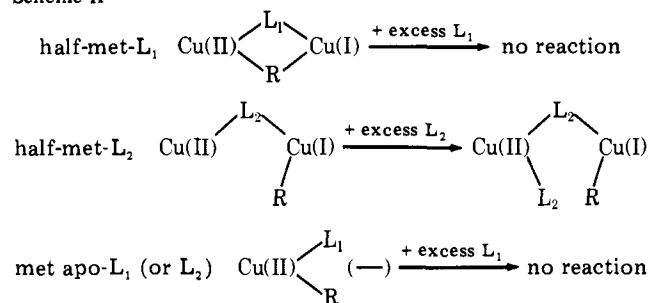


Figure 15. EPR spectra (in pH 6.3 phosphate buffer, 77 K) of (a) half-met-aquo and (b) met apo-aquo.

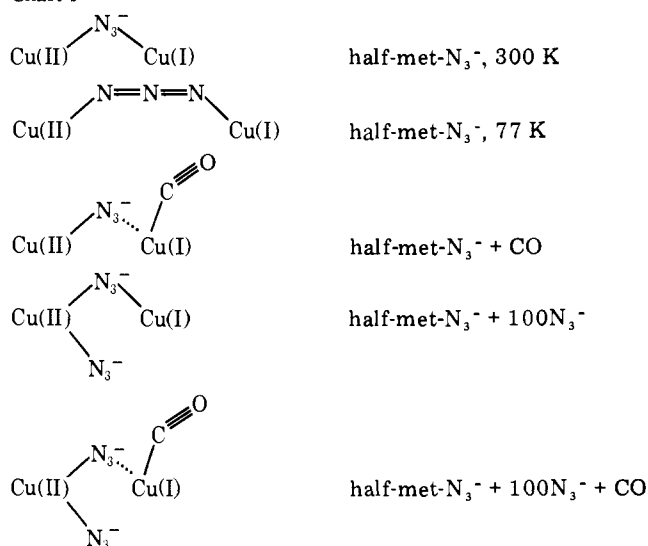
#### Scheme II



generation of a large bridging ligand (via a coupling product) that forces the metals apart. This 6 Å would again be too large to sustain an endogenous protein bridge and the rupture of this bridge would eliminate an effective pathway for antiferromagnetic exchange interactions between the Cu(II)'s. This scheme and steric requirements are consistent with a number of potential protein bridges,<sup>28</sup> in particular, carboxylate and phenolate. While histidine has been indicated by both chemical and spectroscopic evidence<sup>3a,29</sup> to be a ligand at the copper site, it is unlikely that histidine supplies the bridge between the two coppers since imidazole bridging<sup>30</sup> yields a metal-metal distance of  $\sim 6$  Å. Alternatively, it is possible that two different coppers are oxidized in the half-met and met apo derivatives, or that bridging of the exogenous ligand to the Cu(I) in half-met-L forms could distort the coordination geometry of the Cu(II) site, making it accessible to coordination by an additional ligand. A detailed spectroscopic comparison between the met apo-L and half-met-L series is presently under way to distinguish between these possibilities. The spectroscopic results on the half-met derivatives presented here can now be used to determine the bridging geometry of a variety of exogenous ligands to this intermediate oxidized active site.

The spectral features associated with well-defined chemical perturbations on the half-met- $\text{N}_3^-$  derivatives provide a detailed experimental picture of small molecule binding to this active site. First, the half-met- $\text{N}_3^-$  has quite low-energy d-d (relative to the other half-met derivatives) and  $\text{N}_3^- \rightarrow \text{Cu(II)}$  charge-transfer transitions which shift to significantly higher energy upon cooling, signifying a temperature-dependent distortion of the ligands at the Cu(II) site. The low-temperature form is associated with a unique EPR spectrum and the appearance of a reasonably intense transition in the near IR. These spectral features combined with the continued presence of ligand field transitions of the Cu(II) define this half-met- $\text{N}_3^-$  derivative as a class II mixed valence<sup>26</sup> system with the near-IR transition being a Cu(II)Cu(I)  $\rightarrow$  Cu(I)Cu(II) intervalence-transfer transition. The intensity of this transition requires an effective pathway for electron transfer between the two coppers supporting an end-to-end bridging geometry for the low-temperature half-met- $\text{N}_3^-$  derivative and a Cu(II)-

Chart I



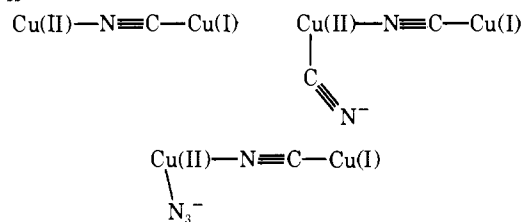
Cu(I) distance of  $\sim 5.1$  Å.<sup>31</sup> As the azide also bridges in the room temperature form of half-met- $N_3^-$  (based on tight binding from dialysis experiments and the presence of an  $N_3^- \rightarrow Cu(II)$  charge-transfer transition at room temperature), which exhibits no spectral properties associated with electron delocalization, the temperature effect must result in a significantly better pathway for electron delocalization. The similar shift in energy of both the d-d and  $N_3^- \rightarrow Cu$  CT transition requires an increase in the tetragonal distortion of the Cu(II) site increasing the energy of the  $d_{x^2-y^2}$  orbital and allowing better  $\pi$  overlap of the  $N_3^-$  with this  $d_{x^2-y^2}$  orbital. Resonance Raman experiments are presently underway to clarify the details of this distortion.

While the  $N_3^-$  is bound less tightly upon coordination of the CO, the  $N_3^- \rightarrow Cu(II)$  charge-transfer transition remains. Thus, while the CO has greatly weakened or broken the  $N_3^-$ -Cu(I) bond, the  $N_3^-$  remains coordinated to the Cu(II). Addition of excess  $N_3^-$  to half-met- $N_3^-$  results in the appearance of a second  $N_3^- \rightarrow Cu(II)$  charge-transfer transition at higher energy than the 490-nm band associated with the bridging azide. The energy and intensity of this charge transfer transition are comparable to that of the  $N_3^- \rightarrow Cu(II)$  charge-transfer transition for the unbridged  $N_3^-$  in met apo- $N_3^-$ . Thus, the second  $N_3^-$  is also coordinating to the Cu(II) without significantly affecting the first  $N_3^-$  (however, the temperature effect no longer occurs, suggesting the Cu(II) ligation is more rigid with the second  $N_3^-$  coordinated).

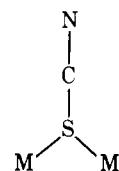
The energies observed for the  $N_3^- \pi^* \rightarrow Cu(II)$   $d_{x^2-y^2}$  CT transition require further comment. The CT transitions associated with the met apo- $N_3^-$  and the excess  $N_3^-$  on the half-met- $N_3^-$  are at very similar energies (420 and 410 nm, respectively), consistent with those reported for azide complexes of copper(II).<sup>32</sup> The CT transition associated with the first azide on half-met- $N_3^-$ , however, occurs at lower energy (490 nm) and with reduced intensity ( $\epsilon < 10^3$  M<sup>-1</sup> cm<sup>-1</sup>). This low energy and intensity provide further confirmation of the role of this azide in bridging the two coppers. Coordination to the Cu(I) is expected to place steric requirements on the  $N_3^-$  coordination to the Cu(II). This would reduce the bonding overlap of the  $N_3^- \pi^*$  with the Cu(II)  $d_{x^2-y^2}$  orbital and thus lower both the energy and intensity of the  $N_3^- \pi^* \rightarrow Cu(II)$   $d_{x^2-y^2}$  CT transition. Finally, both azides are observed to remain coordinated to the Cu(II) upon reacting half-met- $N_3^-$  in excess azide with CO as both charge-transfer transitions remain. These spectral observations lead to the ligand binding modes summarized in Chart I.

It was expected that the CT spectra would directly distin-

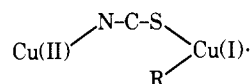
Chart II



guish between the possible bridging isomers of thiocyanate, M-NCS-M' or



in half-met-SCN<sup>-</sup>. However, complications due to oxy-hemocyanin contamination mentioned in the Results section preclude this approach. Alternatively, thiocyanate is generally found to bridge in an end-to-end mode with the linkage isomerization in agreement with hard and soft bonding arguments.<sup>33</sup> The expected coordination in half-met-SCN<sup>-</sup> is then:

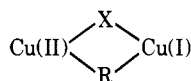


The Cu(II)-Cu(I) distance for this active-site structure should be approximately 5.3 Å by comparison to known inorganic complexes.<sup>34,35</sup> The ability of half-met-SCN<sup>-</sup> to bind a second SCN<sup>-</sup> is consistent with this distance as the previous arguments would classify half-met-SCN<sup>-</sup> along with half-met- $N_3^-$  and half-met-CN<sup>-</sup> as having the exogenous bridge force the coppers too far apart ( $>5$  Å) to sustain a second protein bridge.

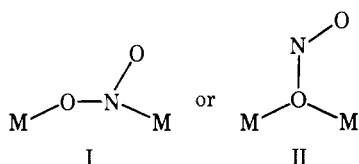
The superhyperfine effects of <sup>13</sup>C labeling for the cyanide derivatives provide an extremely sensitive probe of the mode of coordination of the CN<sup>-</sup> as observable effects are only to be expected for <sup>13</sup>C coordination to the  $d_{x^2-y^2}$  orbital of the Cu(II) site. Figure 10 demonstrates that no broadening of the parallel copper hyperfine lines is observed for the bridging CN<sup>-</sup> in half-met-CN<sup>-</sup> upon labeling. This is extremely reasonable in that CN<sup>-</sup> is only known to bridge linearly as M-C≡N-M and the carbon end should be coordinated to the Cu(I) eliminating any significant Fermi contact of the carbon nucleus with the Cu(II). A Cu(II)-Cu(I) distance of 5.0-5.2 Å is to be expected with this bridging geometry.<sup>37,38</sup> The excess cyanide, however, exhibits superhyperfine broadening, demonstrating carbon coordination to the copper(II). This is to be expected for an unbridged CN<sup>-</sup>, and, in fact, also occurs for the met apo-CN<sup>-</sup> shown by the <sup>13</sup>C superhyperfine broadening for this derivative. The large shift to higher energy of the ligand field transitions upon coordination of the second cyanide is also consistent with this mode of binding. Coordination of  $N_3^-$  to half-met-CN<sup>-</sup> produces spectral changes indicating ligation of the  $N_3^-$  to the Cu(II). Ligand binding of the half-met-CN<sup>-</sup> is summarized in Chart II.

The half-met-halides have produced a wealth of spectroscopic information providing detailed insight into the interaction between the two metals through the halide bridge. First, the very weak binding of F<sup>-</sup> to half-met, the lack of any dominant new features in the absorption spectrum, and the normal Cu(II) EPR spectrum all demonstrate that the F<sup>-</sup> is ineffective as a bridge. For half-met-X, where X = Cl<sup>-</sup>, Br<sup>-</sup>, and I<sup>-</sup>, however, unique spectral features are observed (intense absorption bands in the near-IR and delocalized EPR spectra)

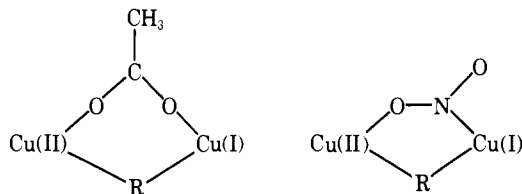
which classify these derivatives along with half-met- $\text{N}_3^-$  (low temperature) as class II mixed valence systems.<sup>26</sup> The variation in these features with X, coupled with the tight binding of the halides to the half-met site, all require a bridging geometry for the halide. The complexity of the copper hyperfine pattern in the  $g_{\parallel}$  EPR spectral region, which is indicative of the rate of thermal exchange between the coppers, is observed to increase for the half-met-X derivatives in an order which parallels the known inner sphere electron transfer rates for these ligands ( $\text{Cl}^- < \text{Br}^- < \text{I}^-$ ).<sup>39</sup> The trends observed for the IT transitions are also consistent with the electron delocalization being through a halide bridge. The energy of the IT transition is observed to decrease and its intensity to increase with increasing rate of electron transfer as expected from the model of Hush.<sup>40</sup> For the halide to provide a resonance pathway for electron exchange through p orbitals, a Cu(II)-X-Cu(I) bond angle somewhat greater than  $90^\circ$  is required.<sup>41</sup> Using average bond lengths from the literature ( $\sim 2.4 \text{ \AA}$ )<sup>42</sup> and a reasonable angle for delocalization through the halide bridge ( $110^\circ$ ), a Cu(II)-Cu(I) distance of less than  $4 \text{ \AA}$  is expected. This distance would also be consistent with the inability of half-met halide forms to coordinate a second exogenous ligand based on retention of a protein bridge as shown below.



The EPR and optical spectra of half-met- $\text{CH}_3\text{CO}_2^-$  and half-met- $\text{NO}_2^-$  indicate binding of only one exogenous ligand at the active site (no change in spectra upon addition of excess ligand). Bridging by an acetate ligand would place the Cu(II)-Cu(I) distance<sup>43</sup> at  $< 3 \text{ \AA}$ . The nitrite ligand has two confirmed bridging modes:<sup>44</sup>



Mode I yields M-M distances of  $\sim 3.6 \text{ \AA}$ , while mode II predicts a smaller M-M distance of  $\sim 3 \text{ \AA}$ . Both are consistent with the lack of any change in the superhyperfine splitting when  $\text{Na}^{15}\text{NO}_2$  was used<sup>20,45</sup> to prepare half-met- $\text{NO}_2^-$ . While bridging mode II cannot be ruled out, mode I is favored due to its more frequent appearance in transition metal complexes. Thus, a reasonable description of the ligand bridging in half-met- $\text{CH}_3\text{CO}_2^-$  and half-met- $\text{NO}_2^-$  is as follows.



Recent studies on binuclear copper model complexes seem to be quite relevant to half-met hemocyanin chemistry. In particular, while no Cu(II)-CO complexes are known, a number of Cu(I)-CO complexes have been prepared and two have been structurally characterized.<sup>46</sup> Although deoxy-hemocyanin binds CO in the stoichiometry of  $1 \text{ CO}/2 \text{ Cu(I)}$ ,<sup>47</sup> the reactions of half-met with CO demonstrate that only one Cu(I) is required for CO coordination at the hemocyanin active site. In fact, a Cu(II)-Cu(I) complex has now been shown to bind CO as an additional ligand<sup>48</sup> (five coordinate at the Cu(I)). The dependence of the half-met + CO reactions on the nature of the bridging ligand and the effects of CO coordination on the stability of this bridge are quite unique and warrant

further investigation. Additionally, half-met hemocyanin represents a stable one-electron intermediate in the two-electron oxidation of the binuclear cuprous active site, as this site is physiologically involved in the  $2e^-$  reduction of  $\text{O}_2$  to  $\text{O}_2^{2-}$ . The stability of this mixed valence state, however, is not surprising in light of recent electrochemical studies on model systems.<sup>49</sup> The mixed valence Cu(II)-Cu(I) oxidation state seems to be generally accessible and only recently has a complex appeared which is capable of sequential two-electron transfer at the same potential.<sup>50</sup> Finally, the active site proposed in an earlier report<sup>51</sup> is consistent with our results demonstrating peroxide and endogenous protein-ligand bridging.

The chemical perturbation-spectroscopic approach contained in this paper yielded information concerning the nature of the active site of a mollusc hemocyanin. We have now generated parallel derivatives of arthropod hemocyanin and *Neurospora* tyrosinase<sup>52</sup> and have observed significant differences among these forms. Spectroscopic studies on these derivatives are presently underway to obtain similar insight into the active site of each of these metalloproteins, and how this site varies over this series which exhibits large differences in their physiological function.

**Acknowledgments.** We are grateful to the National Institute of Arthritis, Metabolism, and Digestive Diseases of the U.S. Public Health Service (AM20406) for support of this research program. Acknowledgment is made to the Alfred P. Sloan Foundation (E.I.S.) and the Whitaker Health Sciences Fund (N.C.E.) for research fellowships.

## References and Notes

- (1) R. Lontie and L. Vanquickenborne in "Metal Ions in Biological Systems", Vol. 3, H. Sigel, Ed., Marcel Dekker, New York, 1974, pp 183-200.
- (2) K. E. van Holde and E. F. J. van Bruggen in "Subunits in Biological Systems", Part A, S. N. Timasheff and G. D. Fasman, Eds., Marcel Dekker, New York, 1971, pp 1-53.
- (3) (a) E. I. Solomon, D. M. Dooley, R. H. Wang, H. B. Gray, M. Cerdonio, F. Mogno, and G. L. Romani, *J. Am. Chem. Soc.*, **98**, 1029 (1976); (b) D. M. Dooley, R. A. Scott, J. Ellinghaus, E. I. Solomon, and H. B. Gray, *Proc. Natl. Acad. Sci. U.S.A.*, **75**, 3019 (1978).
- (4) K. E. van Holde, *Biochemistry*, **6**, 93 (1967).
- (5) (a) T. B. Freedman, J. S. Loehr, and T. M. Loehr, *J. Am. Chem. Soc.*, **98**, 2809 (1976); (b) T. J. Thamann, J. S. Loehr, and T. M. Loehr, *ibid.*, **99**, 4187 (1977).
- (6) L. Vaska, *Acc. Chem. Res.*, **9**, 175 (1976).
- (7) G. Felsenfeld and M. P. Printz, *J. Am. Chem. Soc.*, **81**, 6259 (1959).
- (8) R. Witters and R. Lontie, *FEBS Lett.*, **60**, 400 (1975).
- (9) R. S. Himmelwright, N. C. Eickman, and E. I. Solomon, *Biochem. Biophys. Res. Commun.*, **86**, 628 (1979).
- (10) N. Makino, H. van der Deen, P. McMahlil, D. C. Gould, T. H. Moss, C. Simo, and H. S. Mason, *Biochim. Biophys. Acta*, **532**, 315 (1978).
- (11) R. Witters, M. DeLey, and R. Lontie in "Structure and Function of Hemocyanin", J. V. Bannister, Ed., Springer-Verlag, Berlin, 1977, pp 239-244.
- (12) K. Heirwegh, V. Blaton, and R. Lontie, *Arch. Int. Physiol. Biochim.*, **73**, 149 (1965).
- (13) A. J. M. Schoot Uiterkamp, *FEBS Lett.*, **20**, 93 (1972).
- (14) A. J. M. Schoot Uiterkamp, H. van der Deen, H. C. Berendsen, and J. F. Boas, *Biochim. Biophys. Acta*, **372**, 407 (1974).
- (15) R. S. Himmelwright, N. C. Eickman, and E. I. Solomon, *Biochem. Biophys. Res. Commun.*, **81**, 237 (1978).
- (16) R. S. Himmelwright, N. C. Eickman, and E. I. Solomon, *Biochem. Biophys. Res. Commun.*, **81**, 243 (1978).
- (17) R. S. Himmelwright, N. C. Eickman, and E. I. Solomon, *Biochem. Biophys. Res. Commun.*, **84**, 300 (1978).
- (18) L. Waxman, *J. Biol. Chem.*, **250**, 3796 (1975).
- (19) R. Lontie, V. Blaton, M. Albert, and B. Peeters, *Arch. Int. Physiol. Biochim.*, **73**, 150 (1965).
- (20) H. van der Deen and H. Hoving, *Biochemistry*, **16**, 3519 (1977).
- (21) F. Kubowitz, *Z. Biochem.*, **299**, 32 (1938).
- (22) See, for example, P. H. Haffner and J. E. Coleman, *J. Biol. Chem.*, **250**, 996 (1975).
- (23) The EPR spectra of half-met-aquo and met apo-aquo are pH dependent; thus the EPR spectrum of the met apo-aquo derivative at pH 6.3 phosphate buffer is comprised of a mixture of two forms.
- (24) A. E. Martell and L. G. Sillen, *Chem. Soc., Spec. Publ.*, No. 17 (1964).
- (25) R. Österberg, *Coord. Chem. Rev.*, **12**, 309 (1974).
- (26) M. B. Robin and P. Day, *Adv. Inorg. Chem. Radiochem.*, **10**, 247 (1967).
- (27) T. G. Spiro, personal communication, 1978.
- (28) Sulfur-containing protein ligands (cysteine, methionine, and disulfide) can also be excluded based on the lack of CT transitions expected for these

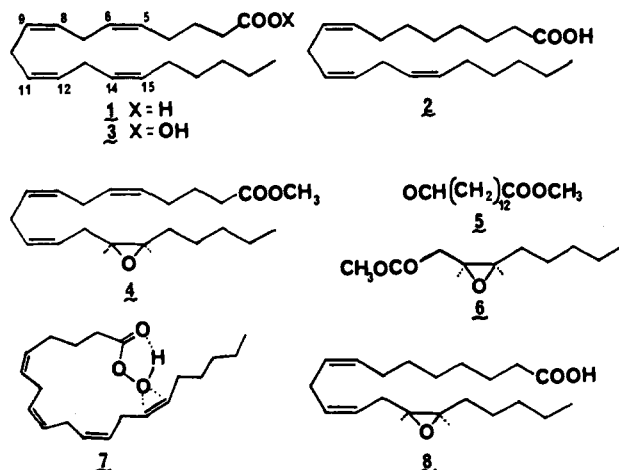
- ligands in the optical spectra.
- (29) (a) B. Salvato, A. Ghirelli-Magaldi, and F. Ghirelli, *Biochemistry*, **13**, 4778 (1974); (b) J. A. Larrabee, T. G. Spiro, N. S. Ferris, W. H. Woodruff, W. A. Maltese, and M. S. Kerr, *J. Am. Chem. Soc.*, **99**, 1979 (1977).
- (30) (a) J. S. Richardson, K. A. Thomas, B. H. Rubin, and D. C. Richardson, *Proc. Natl. Acad. Sci. U.S.A.*, **72**, 1349 (1975); (b) G. Kolks and S. J. Lippard, *J. Am. Chem. Soc.*, **99**, 5804 (1977).
- (31) (a) Z. Dori and R. Ziolo, *Chem. Rev.*, **73**, 247 (1973); (b) T. R. Felthouse and D. N. Hendrickson, *Inorg. Chem.*, **17**, 444 (1978); (c) R. F. Ziolo, A. P. Gaughan, Z. Dori, C. G. Pierpont, and R. Eisenberg, *ibid.*, **10**, 1289 (1971).
- (32) W. Beck, W. P. Fehlhammer, P. Pöllmann, E. Schuierer, and K. Feldl, *Chem. Ber.*, **100**, 2335 (1967).
- (33) J. Nelson and S. M. Nelson, *J. Chem. Soc. A*, 1597 (1969).
- (34) A. H. Norbury, *Adv. Inorg. Chem. Radiochem.*, **17**, 231 (1975).
- (35) (a) A. P. Gaughan, R. F. Ziolo, and Z. Dori, *Inorg. Chim. Acta*, **4**, 640 (1970); (b) J. Garaj, *Inorg. Chem.*, **8**, 304 (1969).
- (36) F. A. Cotton and G. Wilkinson, "Advanced Inorganic Chemistry", 3rd ed., Wiley-Interscience, New York, 1972, p 722.
- (37) (a) W. E. Hatfield and R. Whyman, *Transition Met. Chem.*, **4**, 47 (1969); (b) B. M. Chadwick and A. G. Sharpe, *Adv. Inorg. Chem. Radiochem.*, **8**, 83 (1966).
- (38) (a) D. T. Cromer, *J. Phys. Chem.*, **61**, 1388 (1957); (b) A. Weiss and W. Rothenstein, *Angew. Chem., Int. Ed. Engl.*, **2**, 396 (1963).
- (39) F. Basolo and R. G. Pearson, "Mechanisms of Inorganic Reactions", Wiley, New York, 1967, pp 479-487.
- (40) N. S. Hush, *Prog. Inorg. Chem.*, **8**, 391 (1967).
- (41) W. E. Hatfield in "Extended Interactions Between Metal Ions in Transition Metal Complexes", L. V. Interrante, Ed., American Chemical Society, Washington, D.C., 1974, pp 108-141.
- (42) (a) R. D. Willett, C. Dwiggin, Jr., R. F. Kruh, and R. E. Rundle, *J. Chem. Phys.*, **38**, 2429 (1963); (b) R. D. Willett and C. Chow, *Acta Crystallogr. Sect. B*, **30**, 207 (1974); (c) L. Helmholz, *J. Am. Chem. Soc.*, **69**, 886 (1947); (d) F. Hanic, *Acta Crystallogr.*, **12**, 739 (1959); (e) V. C. Copeland, P. Singh, W. E. Hatfield, and D. J. Hodgson, *Inorg. Chem.*, **11**, 1826 (1972).
- (43) (a) J. N. Van Niekerk and F. R. L. Schoening, *Acta Crystallogr.*, **6**, 227 (1953); (b) C. B. Acland and H. C. Freeman, *Chem. Commun.*, 1016 (1971).
- (44) (a) D. M. L. Goodgame, M. A. Hitchman, D. F. Marsham, P. Phavanantha, and D. Rogers, *Chem. Commun.*, 1383 (1969); (b) M. G. B. Drew, D. M. L. Goodgame, M. A. Hitchman, and D. Rogers, *ibid.*, 477 (1965).
- (45) R. S. Himmelwright, N. C. Eickman, and E. I. Solomon, unpublished results.
- (46) (a) F. A. Cotton and T. J. Marks, *J. Am. Chem. Soc.*, **92**, 5114 (1970); (b) R. Mason and G. Rucci, *Chem. Commun.*, 1132 (1971); (c) G. Rucci, C. Zanzottera, M. P. Lachi, and M. Camia, *ibid.*, 652 (1971); (d) R. R. Gagné, J. L. Allison, R. S. Gall, and C. A. Koval, *J. Am. Chem. Soc.*, **99**, 7170 (1977); (e) M. R. Churchill, B. G. DeBoer, F. J. Rotella, O. M. Abu Salah, and M. I. Bruce, *Inorg. Chem.*, **14**, 2051 (1975).
- (47) C. Bonaventura, B. Sullivan, J. Bonaventura, and S. Bourne, *Biochemistry*, **13**, 4784 (1974).
- (48) R. R. Gagné, C. A. Koval, and T. J. Smith, *J. Am. Chem. Soc.*, **99**, 8367 (1977).
- (49) A. W. Addison, *Inorg. Nucl. Chem. Lett.*, **12**, 899 (1976).
- (50) D. E. Fenton, R. R. Schroeder, and R. L. Lintvedt, *J. Am. Chem. Soc.*, **100**, 1931 (1978).
- (51) A. R. Amundsen, J. Whelan, and B. Bosnich, *J. Am. Chem. Soc.*, **99**, 6730 (1977).
- (52) K. Lerch, R. S. Himmelwright, N. C. Eickman, and E. I. Solomon, manuscript in preparation.

## Communications to the Editor

### Selective Epoxidation of Eicosa-*cis*-5,8,11,14-tetraenoic (Arachidonic) Acid and Eicosa-*cis*-8,11,14-trienoic Acid

Sir:

The key role of arachidonic acid (**1**) as the predecessor of a large family of biologically important substances including prostaglandins (PG's), thromboxanes, SRS-A, HETE, and prostacyclin (members of the "arachidonic cascade"<sup>1</sup>) depends on highly selective enzymatic oxidation of this substrate as a primary event. Similarly, selective oxidation of eicosa-*cis*-8,11,14-trienoic acid (**2**) initiates the series of transformations leading to PG<sub>1</sub> derivatives. Despite the great interest in such controlled biological oxidations of **1** and **2**, and despite the obvious utility of the primary oxidation products as intermediates for the synthesis of various metabolites of **1** and **2**, there has been no demonstrated example of selective *chemical* oxidation of these polyunsaturated substrates. This communication describes the first successful approach to this chemical



problem, specifically new methodology for epoxidation of either the double bond *closest* or *farthest* from the carboxyl function of **1** or **2**.

Direct epoxidation of **1** or **2**, or their esters, by peroxy acid reagents, e.g., *m*-chloroperoxybenzoic acid, is essentially nonselective and leads to a mixture of all possible oxides.<sup>2</sup> In contrast, *internal* epoxidation of **1** or **2** under the proper conditions has now been found to be *highly* selective.

The preparation of peroxyarachidonic acid (**3**) by previously detailed methods proved to be elusive. However, it was possible to generate solutions of this self-reactive intermediate by the following new method. A solution of *pure* (>99%) **1** in dry methylene chloride was allowed to react with 1.05 equiv of carbonyldiimidazole at 25 °C for 20 min to form arachidonylimidazole and this solution was added over 2 min to a cold (0 °C), anhydrous solution (~3.5 M) of hydrogen peroxide (20 equiv) in ether containing 0.01 equiv of lithium imidazolide as basic catalyst.<sup>3</sup> After 3-min stirring, additional methylene chloride was added along with 15 equiv of finely powdered anhydrous potassium bisulfate and the resulting mixture was stirred for 3 min.<sup>4</sup> Separation of the cloudy supernatant solution and addition of anhydrous sodium sulfate provided a dry solution of the peroxy acid **3**.<sup>5</sup>

Upon standing at 20 °C, the peroxy acid **3** gradually was transformed into a more polar product which showed a slightly lower *R<sub>f</sub>* than **1**. Esterification of the reaction product with diazomethane gave after isolation >98% yield of essentially pure<sup>6</sup> epoxy ester **4**.<sup>7</sup> The structure of **4** was ascertained by catalytic hydrogenation (in tetrahydrofuran (THF) over Pd/C catalyst at 1 atm) to the saturated epoxy ester and subsequent cleavage with periodic acid in aqueous THF (or alternatively in two steps with (a) perchloric acid-water-dimethoxyethane for glycol formation and (b) lead tetraacetate) to give in 85% yield (after extractive isolation) the ester aldehyde **5** which was fully characterized by <sup>1</sup>H NMR, IR, and mass spectra and by oxidation (dichromate) and esterification (CH<sub>2</sub>N<sub>2</sub>) to dimethyl 1,12-tetradecanedioate (compared with an authentic